An efficient approach to the numerical solution of rate-independent problems with nonconvex energies

Sören Bartels[a] *& Martin Kružík*[b]

[a]Institut für Numerische Simulation, Rheinische Friedrich-Wilhelms-Universität Bonn, Wegelerstraße 6, D-53115 Bonn, Germany

[b] Institute of Information Theory and Automation of the ASCR, Pod vodárenskou věží 4, 182 08 Prague, Czech Republic, and Czech Technical University, Faculty of Civil Engineering, Thákurova 7, 166 29 Prague, Czech Republic

Abstract. We propose a new approach to the numerical treatment of non(quasi)convex rate-independent evolutionary problems. The main idea is to replace the non(quasi)convex energy density by its polyconvexification. For this problem, first-order optimality conditions are derived and used in finding a discrete solution. The effectiveness of the method is illustrated with some numerical experiments.

Key words. nonconvexity, numerical solution, rate-independent problems

AMS (MOS) subject classification. 49J45

1. Introduction - the underlying mathematical model

The aim of this contribution is to propose a computational method for solving non(quasi)convex vectorial and multidimensional variational problems. It is well known that if $V(y) := \int_\Omega W(\nabla y(x)) \, dx$ where $\Omega \subset \mathbb{R}^n$ is a bounded Lipschitz domain and $W : \mathbb{R}^{m \times n} \to \mathbb{R}$ is continuous but not quasiconvex then V is not weakly sequentially lower semicontinuous on $W^{1,p}(\Omega; \mathbb{R}^m)$, $1 < p < +\infty$, and consequently V does not necessarily attain its minimum in this space. We recall that $W : \mathbb{R}^{m \times n} \to \mathbb{R}$ is quasiconvex if for all $\psi \in W_0^{1,\infty}(\Omega; \mathbb{R}^m)$ and all $F \in \mathbb{R}^{m \times n}$ it holds that

$$
(1) \qquad W(F)|\Omega| \leq \int_\Omega W(F + \nabla\psi(x)) \, dx \ .
$$

One way, how to overcome this difficulty is to replace W by its quasiconvex envelope QW defined as the pointwise supremum of all quasiconvex functions not greater than W, cf. [10]. This is, however, mostly a theoretical tool because the formula is generically not known in a closed form. Nevertheless, by the relaxation theorem [10] we have $\inf_y \int_\Omega W(\nabla y(x)) \, dx = \min_y \int_\Omega QW(\nabla y(x)) \, dx$. In this paper we suggest to work with the polyconvex envelope PW instead. The polyconvex envelope is defined analogously to the quasiconvex one and we say that W is polyconvex [4, 10] if there is a convex function $h : \mathbb{R}^\sigma \to \mathbb{R}$ such that $W(F) = h(\mathbb{T}(F))$ for all $F \in \mathbb{R}^{m \times n}$. Here $\mathbb{T}(F)$ denotes the vector

of all subdeterminants of F, i.e., the dimension of $\mathbb{T}(F)$ equals

$$(2) \qquad \sigma := \sum_{k=1}^{\min(m,n)} \binom{m}{k}\binom{n}{k} = \binom{m+n}{n} - 1 \ .$$

Polyconvexity implies quasiconvexity and it is a stronger property if $\min(m,n) > 1$. The resulting variational problem $\min_y \int_\Omega PW(\nabla y(x))\,\mathrm{d}x$ is well-posed and we have

$$\inf_y \int_\Omega W(\nabla y(x))\,\mathrm{d}x = \min_y \int_\Omega QW(\nabla y(x))\,\mathrm{d}x \geq \min_y \int_\Omega PW(\nabla y(x))\,\mathrm{d}x \ ,$$

where the last inequality can be strict in particular cases. The advantage is that there are efficient numerical methods to evaluate $PW(F)$ [8, 24]. There is another widely used method to estimate QW, namely the so-called rank-one convexification of W. The function W is called rank-one convex if it is convex between points in $\mathbb{R}^{m\times n}$ whose difference is a rank-one matrix. Estimating the rank-one convex envelope of W by so-called laminates [23] in the context of elasticity is used e.g. in [3, 15, 14, 18]. In these cases, W is the stored energy density of a hyperelastic material. We recall that laminates are among experimentally observed material microstructures. Algorithms for the approximation of the rank-one convex envelope have been proposed and analyzed in [11, 7]. Unfortunately, they are extremely expensive and may lead to ill-posed, i.e., non-weakly lower semicontinuous, variational problems.

The supremum definitions of QW or PW mentioned above are not very useful for numerical or analytical considerations. Much more suitable ways how to evaluate them were developed in terms of parameterized (Young) measures.

1.1. **Young measures.** It is well known [5] that if $\{z_k\}_{k\in\mathbb{N}} \subset L^p(\Omega;\mathbb{R}^{m\times n})$, $1 \leq p < +\infty$, is bounded then there exists a subsequence (not relabeled) and a family $\nu = \{\nu_x\}_{x\in\Omega}$ of probability measures on Ω such that for all $g \in L^\infty(\Omega)$ and all $f \in C(\mathbb{R}^{m\times n})$ such that $\{f(z_k)\}_{k\in\mathbb{N}}$ is uniformly integrable in $L^1(\Omega)$ it holds that

$$(3) \qquad \lim_{k\to\infty} \int_\Omega f(z_k(x))g(x)\,\mathrm{d}x = \int_\Omega \int_{\mathbb{R}^{m\times n}} f(s)\nu_x(\mathrm{d}s)g(x)\,\mathrm{d}x \ .$$

Conversely, if $\nu = \{\nu_x\}_{x\in\Omega}$ is such that ν_x is for almost all $x \in \Omega$ a probability measure on $\mathbb{R}^{m\times n}$, $x \mapsto \int_{\mathbb{R}^{m\times n}} f(s)\nu_x(\mathrm{d}s)$ is measurable for all $f \in C_0(\mathbb{R}^{m\times n})$, and $\int_\Omega \int_{\mathbb{R}^{m\times n}} |s|^p \nu_x(\mathrm{d}s)\,\mathrm{d}x < +\infty$ then there exists a sequence $\{z_k\}_{k\in\mathbb{N}} \subset L^p(\Omega;\mathbb{R}^{m\times n})$ such that (3) holds. The family $\nu = \{\nu_x\}$ is called Young measure and $\{z_k\}$ its generating sequence. It is well-known that every Young measure ν as above can be generated by a sequence $\{z_k\}$ such that $\{f(z_k)\}$ is uniformly integrable for every continuous $f \in C_p(\mathbb{R}^{m\times n}) := \{f \in C(\mathbb{R}^{m\times n}); |f| \leq C(1 + |\cdot|^p), \ C > 0\}$.

We will be interested in Young measures generated by gradients, i.e. $z_k := \nabla y_k$ for some sequence $\{y_k\} \subset W^{1,p}(\Omega;\mathbb{R}^m)$. Such a Young measure will be refered to as gradient Young measure. Fixing $1 \leq p < +\infty$, we denote the set of gradient Young measures generated by $\{\nabla y_k\}$ for $\{y_k\} \subset W^{1,p}(\Omega;\mathbb{R}^m)$ by $\mathbb{G}^p(\Omega;\mathbb{R}^{m\times n})$. Thus, if

$\{y_k\} \subset W^{1,p}(\Omega; \mathbb{R}^m)$ is bounded and $\{W(\nabla y_k)\}$ equiintegrable, we have (up to a subsequence) that $\lim_{k \to \infty} V(y_k) = \int_\Omega \int_{\mathbb{R}^{m \times n}} W(s)\nu_x(ds)$. Let us mention that if W is coercive with superlinear growth at infinity and $\{y_k\}$ is minimizing for V then the equiintegrability condition holds. The following well-known result of Kinderlehrer and Pedregal [23] characterizes the set of gradient Young measures.

Lemma 1.1. *Let* $1 < p < +\infty$. *A Young measure* $\nu = \{\nu_x\}_{x \in \Omega}$ *belongs to* $\mathbb{G}^p(\Omega; \mathbb{R}^{m \times n})$ *if and only if the following three conditions are satisfied simultaneously:*
(i) there is $y \in W^{1,p}(\Omega; \mathbb{R}^n)$ *such that for a.a.* $x \in \Omega$

$$(4) \qquad \nabla y(x) = \int_{\mathbb{R}^{m \times n}} s\nu_x(dF) ,$$

(ii) for this y *and all quasiconvex functions* $v : \mathbb{R}^{m \times n} \to \mathbb{R}$, $|v| \leq C(1 + |\cdot|^p)$, *it holds that for a.a.* $x \in \Omega$

$$(5) \qquad v(\nabla y(x)) \leq \int_{\mathbb{R}^{m \times n}} v(F)\nu_x(dF) ,$$

(iii) it holds that

$$(6) \qquad \int_\Omega \int_{\mathbb{R}^{m \times n}} |F|^p \nu_x(dF)\, dx < +\infty .$$

Extending the validity of (ii) to all rank-one convex functions with p-growth at infinity defines a subset of $\mathbb{G}^p(\Omega; \mathbb{R}^{m \times n})$ called laminates [23].

In this paper, we propose a different approach, namely to use a proper supset of $\mathbb{G}^p(\Omega; \mathbb{R}^{m \times n})$ by requiring that (5) holds only for all quasiaffine functions. We recall that v is quasiaffine if and only if it is an affine function of all subdeterminants of the matrix argument. This means that there is $\pi \in \mathbb{R}^\sigma$ and $c \in \mathbb{R}$ such that $v(\cdot) := \pi \cdot \mathbb{T}(\cdot) + c$. In particular, if $m = n = 2$ then $v(F) := a \cdot F + b\det F + c$ for some $a \in \mathbb{R}^{2 \times 2}$ and $b, c \in \mathbb{R}$. If $n = 3$ then $v(F) := a \cdot F + b \cdot \text{cof} F + c\det F + d$ for some $a, b \in \mathbb{R}^{3 \times 3}$ and $c, d \in \mathbb{R}$. We are going to deal with the following superset of gradient Young measures.

Definition 1.2. *Let* $\min(m, n) < p < +\infty$. *A Young measure* $\nu = \{\nu_x\}_{x \in \Omega}$ *is called polyconvex and belongs to the set* $\mathbb{P}^p(\Omega; \mathbb{R}^{m \times n})$ *if the following conditions are satisfied:*
(i) there is $y \in W^{1,p}(\Omega; \mathbb{R}^n)$ *such that for a.a.* $x \in \Omega$

$$(7) \qquad \mathbb{T}(\nabla y(x)) = \int_{\mathbb{R}^{m \times n}} \mathbb{T}(F)\nu_x(dF) ,$$

(ii) it holds that

$$(8) \qquad \int_\Omega \int_{\mathbb{R}^{m \times n}} |F|^p \nu_x(dF)\, dx < +\infty .$$

Young measures are an important tool in the mathematical treatment of various nonconvex variational problems. A prominent example is the relaxation of energy functionals in the modeling of shape memory materials.

1.2. **Shape memory alloys.** Shape-memory alloys (SMAs) are active materials, and have been the subject of intensive theoretical and experimental research during the past decades. Existing or potential applications can be found, for example, in medicine and mechanical or aerospace engineering. Shape-memory alloys are crystalline materials that exhibit specific hysteretic stress / strain / temperature response; they have the ability to recover a trained shape after deformation and subsequent reheating. This is called the shape-memory effect. It is based on the ability of the alloy to rearrange atoms in different crystallographic configurations (in particular, with different symmetry groups). The stability depends on the temperature. Normally, at higher temperatures a high-symmetry (for example, cubic) lattice is stable, which is referred to as the austenite phase. At lower temperatures, a lattice of lower symmetry (for example, tetragonal, orthorhombic, monoclinic, or triclinic) becomes stable, called the martensite phase. Due to the loss of symmetry, this phase may occur in different variants. The number of variants M, is the quotient of the order of the high-symmetry phase and the order of the low-symmetry group. So for a cubic high-symmetry phase, $M = 3$, 6, 12, or 4 for the tetragonal, orthorhombic, monoclinic, respectively triclinic martensites mentioned above. The variants can be combined coherently with each other, forming so-called twins of two variants.

The mathematical and computational modeling of SMAs represents a tool for the theoretical understanding of phase transition processes in solids. Such an analysis may complement experimental results, predict the response of new materials, or facilitate the usage of SMAs in applications. SMAs are genuine multi-scale materials and create a variety of challenges for mathematical modeling. We refer the reader to [26] for a survey of a wide menagerie of SMA models ranging from nano- to macro-scales. In this article, we focus on a mesoscopic model in the framework of continuum mechanics. Beside the macroscopic deformation and its gradient, the model also involves the volume fractions of phases and variants and gradients of volume fraction. This seems a reasonable compromise, since it allows for the modeling scales of large single crystals or polycrystals.

Although the natural physical dimension is three we will assume that our specimen occupies a bounded domain $\Omega \subset \mathbb{R}^n$ and the deformation y maps Ω to $\mathbb{R}^m$. This allows us to consider various variational problems. Nevertheless for shape memory applications we obviously assume that $m = n = 3$. The stress-free parent austenite is a natural state of the material which makes it, in the context of continuum mechanics, a canonical choice for the reference configuration. As usual, $y \colon \Omega \to \mathbb{R}^m$ denotes the deformation and $u \colon \Omega \to \mathbb{R}^m$ the displacement, which are related to each other via the identity $y(x) = x + u(x)$, where $x \in \Omega$. Hence the deformation gradient is $F := \nabla y = I + \nabla u$.

The total stored energy in the bulk occupying, in its reference configuration, the domain Ω is then

$$(9) \qquad\qquad V(y) := \int_{\Omega} W(\nabla y(x)) \mathrm{d}x.$$

A common variational principle in continuum mechanics is the minimization of the stored energy. Due to the coexistence of several variants at low temperature, W has multiple minima and thus a multi-well character. We consider an isothermal situation with several

coexisting variants. Since W is a multi-well energy density, minimizing sequences of V tend to develop, in general, finer and finer spatial oscillations of their gradients. In other words, the deformation gradient often tends to develop fine spatial oscillations due to lack of (quasi-)convexity of the stored energy density. These oscillations are difficult to model in full detail, although some studies in this direction exist [1]. The oscillations correspond to the development of finer and finer microstructures when the stored energy is to be minimised. The minimum of V, under specific boundary conditions for y, is usually not attained in a space of functions. Therefore one needs to extend the notion of a solution. Young measures are here an appropriate tool. They are capable of recording, on a mesoscopic level, the limit information of the finer and finer oscillating deformation gradient as we move towards the macroscopic scale. This can be described, for a current macroscopic point $x \in \Omega$, by a probability measure ν_x on the set of deformation gradients, that is, matrices in $\mathbb{R}^{n \times n}$.

1.2.1. *Dissipation related to phase transitions.* In order to describe dissipation due to transformations we adopt, following e.g. [20], the standpoint that the amount of dissipated energy associated with a particular phase transition between austenite and a martensitic variant or between two martensitic variants can be described by a specific energy (of the dimension $\mathrm{J/m^3} = \mathrm{Pa}$). This viewpoint has been independently adopted in physics, see [16]. For an explicit definition of the transformation dissipation, we need to identify the particular phases or phase variants. To this behalf, we define a continuous mapping $\mathcal{L}\colon \mathbb{R}^{n \times n} \to \triangle$, where

$$\triangle := \Big\{ \zeta \in \mathbb{R}^{1+M} \ \big| \ \zeta_\ell \geq 0 \text{ for } \ell = 1, \dots, M+1, \text{ and } \sum_{\ell=1}^{M+1} \zeta_\ell = 1 \Big\}$$

is a simplex with $M+1$ vertices, with M being the number of martensitic variants. Here $\mathcal{L}$ is related with the material itself and thus has to be frame indifferent. We assume, beside $\zeta_\ell \geq 0$ and $\sum_{\ell=1}^{M+1} \zeta_\ell = 1$, that the coordinate ζ_ℓ of $\mathcal{L}(F)$ takes the value 1 if F is in the ℓ-th (phase) variant, that is, F is in a vicinity of ℓ-th well $\mathrm{SO}(n)U_\ell$ of W, which can be identified by the stretch tensor $F^\top F$ being close to $U_\ell^\top U_\ell$. If $\mathcal{L}(F)$ is not in any vertex of $\triangle$, then it means that F is in the spinodal region where no definite phase or variant is specified. We assume, however, that the wells are sufficiently deep and the phases and variants are geometrically sufficiently far from each other that the tendency for minimization of the stored energy will essentially prevent F to range into the spinodal region. Thus, the concrete form of $\mathcal{L}$ is not important as long as $\mathcal{L}$ enjoys the properties listed above. We remark that $\mathcal{L}$ plays the rôle of what is often called vector of order parameters or a vector-valued internal variable.

For two states q_1 and q_2, with $q_j = (y_i, \nu_i, \lambda_i)$ for $j = 1, 2$, we now define the dissipation due to martensitic transformation which "measures" changes in the volume fraction $\lambda \in L^\infty\big(\Omega; \mathbb{R}^{M+1}\big)$. This dissipation is given by

$$(10) \qquad \mathcal{D}\left(q_1, q_2\right) := \int_\Omega |\lambda_1(x) - \lambda_2(x)|_{\mathbb{R}^{M+1}} \, \mathrm{d}x \ ,$$

5

where

$$(11) \qquad \lambda_j(x) := \int_{\mathbb{R}^{m \times n}} \mathcal{L}(F) \nu_{j,x}(\mathrm{d}F)$$

and $|\cdot|_{\mathbb{R}^{M+1}}$ is a norm on $\mathbb{R}^{M+1}$. As $\sum_{j=1}^{M+1} \lambda_j = 1$ we call λ the vector-valued volume fraction as it gives us relative portions of variants at almost every $x \in \Omega$.

1.2.2. *Loading and boundary conditions.* In experiments, a specimen occupying the region Ω will be subjected to external loads. In order to simplify our exposition, we consider only surface forces. We assume that there is a spatially constant tensor $S \in \mathbb{R}^{m \times n}$ such that the density of surface forces g applied on $\Gamma_1 \subset \partial\Omega$ is given by $g = S\varrho$, where ϱ is the unit outer normal vector to Γ_1. We also assume that we are given a set $\Gamma_0 \subset \partial\Omega$, where the $(n-1)$-dimensional Hausdorff measure of Γ_0 is positive. We consider Dirichlet boundary conditions $y = y_0$ on Γ_0 for some prescribed (time-dependent/independent) mapping y_0. As for the surface forces we define a linear functional

$$(12) \qquad L(y) := \int_{\Gamma_1} S\varrho \cdot y(x)\mathrm{d}A = \int_{\Omega} S \cdot \nabla y(x)\mathrm{d}x \ .$$

Below, we write $L = L(t,y)$ to indicate the possibility of temporally changing forces g and therefore also S.

1.3. Energetic solution.
Combining the previous considerations, we arrive at the energy functional $\mathcal{I}$ of the form

$$(13) \qquad \mathcal{I}(t,q) := \int_{\Omega} \int_{\mathbb{R}^{m \times n}} (W(F) - S \cdot F)\nu_x(\mathrm{d}F)\mathrm{d}x + \varepsilon \left\| \nabla\lambda \right\|_{L^2\left(\Omega;\mathbb{R}^{(1+M) \times n}\right)} \ .$$

It is often convenient to write

$$(14) \qquad V(q) := \int_{\Omega} \int_{\mathbb{R}^{m \times n}} W(F)\nu_x(\mathrm{d}F)\mathrm{d}x + \varepsilon \left\| \nabla\lambda \right\|_{L^2\left(\Omega;\mathbb{R}^{(1+M) \times n}\right)} \ ,$$

where the $\nabla\lambda$-term is included to regularize the problem. It penalizes spatial jumps of the volume fraction λ and introduces a length scale to the problem depending on a parameter $\varepsilon > 0$.

In what follows, we suppose that there are $c, C > 0$ such that for all $s \in \mathbb{R}^{m \times n}$

$$(15) \qquad c(-1 + |F|^p) \le W(F) \le C(1 + |F|^p)$$

Following [13] we assume that there are constants $C_0, C_1 > 0$ such that

$$(16) \qquad |\partial_t \mathcal{I}(t,q)| \le C_0(C_1 + \mathcal{I}(t,q)) \ .$$

6

Let $\mathfrak{T} > 0$ denote the time horizon. We assume uniform continuity of $t \mapsto \partial_t \mathcal{I}(t, q)$ in the sense that there is $\omega : [0, \mathfrak{T}] \to [0, +\infty)$ nondecreasing such that for all $t_1, t_2 \in [0, \mathfrak{T}]$

$$(17) \qquad |\partial_t \mathcal{I}(t_1, q) - \partial_t \mathcal{I}(t_1, q)| \leq \omega(|t_1 - t_2|) .$$

We also suppose that $q \mapsto \partial_t \mathcal{I}(t, q)$ is wekly continuous for all $t \in [0, \mathfrak{T}]$.

$$(18) \qquad y \in \mathbb{Y}^p (\Omega; \mathbb{R}^m) := \left\{ y \in W^{1,p} (\Omega; \mathbb{R}^m) \mid y = 0 \text{ on } \Gamma_0 \right\} ,$$

where $\Gamma_0 \subset \partial\Omega$ with a positive surface measure, as described in Subsection 1.2.2. Here y_0 is a time-dependent trace on Γ_0 We recall from that subsection that $\Gamma_0 \cap \Gamma_1 = \emptyset$ by assumption. Then we look for $q \in \mathcal{Q} := \mathbb{Y}^p (\Omega; \mathbb{R}^m) \times \mathbb{G}^p (\Omega; \mathbb{R}^{m \times n}) \times W^{1,2}(\Omega; \mathbb{R}^{M+1})$ and restrict the space further by imposing the admissibility condition

$$(19) \qquad \mathbb{Q} := \left\{ q \in \mathcal{Q} \mid \lambda = \mathcal{L} \bullet \nu \text{ and } \nabla y = \mathbb{I} \bullet \nu \right\} ,$$

where, for almost all $x \in \Omega$, $[\mathcal{L} \bullet \nu](x) := \int_{\mathbb{R}^{m \times n}} \mathcal{L}(F)\nu_x(\mathrm{d}F)$; $\mathbb{I} \bullet \nu$ is defined analogously.

Remark 1.3. *If we prescribe time-dependent boundary conditions $y_0(t) \in W^{1,p}(\Omega; \mathbb{R}^m)$ on Γ_0 then we write*

$$(20)$$
$$\mathcal{I}(t, q) := \int_\Omega \int_{\mathbb{R}^{m \times n}} (W(F + \nabla y_0(t, x)) - S \cdot (F + \nabla y_0(t, x))\nu_x(\mathrm{d}F)\mathrm{d}x + \varepsilon \left\| \nabla \lambda \right\|_{L^2\left(\Omega; \mathbb{R}^{(1+M) \times n}\right)} .$$

This allows us to keep $\mathbb{Q}$ independent of time.

We seek to analyze the time evolution of a process $q(t) \in \mathbb{Q}$ during the time interval $[0, \mathfrak{T}]$. The following two properties are key ingredients of the so-called energetic solution introduced by Mielke and Theil [22].

(i) *tability inequality*: for every $t \in [0, \mathfrak{T}]$ and every $\tilde{q} \in \mathbb{Q}$, it holds that

$$(21) \qquad \mathcal{I}(t, q(t)) \leq \mathcal{I}(t, \tilde{q}) + \mathcal{D}(q(t), \tilde{q}) .$$

(ii) *Energy balance*: For every $0 \leq t \leq \mathfrak{T}$,

$$(22) \qquad \mathcal{I}(t, q(t)) + \mathrm{Var}(\mathcal{D}, q; [0, t]) = \mathcal{I}(0, q(0)) + \int_0^t \partial_t \mathcal{I}(\xi, q(\xi))\mathrm{d}\xi ,$$

where

$$\mathrm{Var}(\mathcal{D}, z; [s, t]) := \sup \left\{ \sum_{j=1}^N \mathcal{D}(q(t_{j-1}), q(t_j)) \mid \{t_j\}_{j=0}^N \text{ is a partition of } [s, t] \right\}$$

is the *variation* of the dissipation.

Definition 1.4. *The mapping $q : [0, \mathfrak{T}] \to \mathbb{Q}$ is an* energetic solution *to the problem $(\mathcal{I}, \mathcal{D}, L)$ with the energy functional $\mathcal{I}$ as in (13), the dissipation $\mathcal{D}$ and the load L as in (12) if the stability inequality (21) and energy balance (22) are satisfied for every $t \in [0, \mathfrak{T}]$.*

We aim at proving the following theorem regarding the existence of an energetic solution.

Theorem 1.5. *Let $p > 1$, $S \in C^1([0, \mathfrak{T}]; \mathbb{R}^{m \times n})$, and let assumptions (15), (16), and (17) hold. Then there is a process $q \colon [0, \mathfrak{T}] \to \mathbb{Q}$ with $q(t) = (y(t), \nu(t), \lambda(t))$ such that q is an energetic solution according to Definition 1.4. for a given stable initial condition $q_0 \in \mathbb{Q}$.*

2. Existence of a solution

The proof of Theorem 1.5 relies on approximations by time-discrete (incremental) problems constructed for a given time step. These are minimization problems over spatial variables. Each minimization problem takes into account the solution obtained for the previous time step while the initial condition serves as input for the first minimization problem. Details can be found e.g. in [13].

2.1. **Incremental problems.** The proof of existence of a rate-independent evolution commonly proceeds via time-discretization. Thus, in a first step, a sequence of incremental problems is defined. We define a time discretization $0 = t_0 < \ldots < t_n = \mathfrak{T}$ with a time step $\tau := \max_i(t_i - t_{i-1})$. Let an initial state $\mathbb{S}(0) \ni q_0 =: q_0 \in \mathbb{Q}$ be given. For $1 \leq k \leq N$ we find $q_k \in \mathbb{Q}$ by solving

$$(23) \qquad \text{minimize } \mathcal{I}(t_k, q) + \mathcal{D}(q_{k-1}, q), \text{subject to } q \in \mathbb{Q}.$$

The existence of a solution to the time step problem (23) follows by the direct method of the calculus of variations. Notice that this is true even if $\varepsilon = 0$ and if we consider $\lambda \in L^2(\Omega; \mathbb{R}^{M+1})$ only.

We denote $q \in \mathbb{QP} := \mathbb{Y}^p(\Omega; \mathbb{R}^m) \times \mathbb{P}^p(\Omega; \mathbb{R}^{m \times n}) \times W^{1,2}(\Omega; \mathbb{R}^{M+1})$

$$(24) \qquad \mathbb{P} := \left\{ q \in \mathbb{QP} \mid \lambda = \mathcal{L} \bullet \nu \text{ and } \nabla y = \mathbb{I} \bullet \nu \right\},$$

moreover, clearly $\mathbb{Q} \subset \mathbb{P}$.

Then we can define the following incremental problem: For $1 \leq k \leq N$ we find $q_k \in \mathbb{P}$ by solving

$$(25) \qquad \text{minimize } \mathcal{I}(t_k, q) + \mathcal{D}(q_{k-1}, q), \text{subject to } q \in \mathbb{P}.$$

The existence of a solution to (25) follows again by the direct method of the calculus of variations. Moreover, as proved e.g. in [13], the following two-sided energy estimate hold for $k \geq 1$:

$$(26) \quad \int_{t_{k-1}}^{t_k} \partial_t \mathcal{I}(s, q_k) \, \mathrm{d}s \leq \mathcal{I}(t_k, q_k) + \mathcal{D}(q_{k-1}, q_k) - \mathcal{I}(t_{k-1}, q_{k-1}) \leq \int_{t_{k-1}}^{t_k} \partial_t \mathcal{I}(s, q_{k-1}) \, \mathrm{d}s.$$

Assume that the norm on $\mathbb{R}^{M+1}$ defining the dissipation in (10) is given as follows:

$$(27) \qquad |X|_{\mathbb{R}^{M+1}} := \sum_{i=1}^{M+1} c^i |X^i|, \quad X = (X^1, \ldots, X^{M+1})$$

8

where $|\cdot|$ is the absolute value and $c^i > 0$ for all i. The physical meaning of c^i is the specific energy dissipated if X^i changes from zero to one (or vice versa).

As we are primarily interested in an efficient numerical solution to incremental problems (25) we drop the $\nabla\lambda$-term in (13) by putting $\varepsilon := 0$ and consider the following simplified minimization task:

$$(28) \qquad \text{minimize } \mathcal{I}(t_k, q) + \mathcal{D}(q_{k-1}, q), \text{subject to } q \in \mathbb{P}' \ ,$$

where

$$\mathbb{P}' := \left\{ q \in \mathbb{QP}' \ \middle| \ \lambda = \mathcal{L} \bullet \nu \text{ and } \nabla y = \mathbb{I} \bullet \nu \right\} \ ,$$

with $\mathbb{QP}' := \mathbb{Y}^p (\Omega; \mathbb{R}^m) \times \mathbb{P}^p(\Omega; \mathbb{R}^{m\times n}) \times L^2(\Omega; \mathbb{R}^{M+1})$.

In other words, having q_{k-1} we look for $q_k \in \mathbb{QP}'$ which minimizes

$$(29) \qquad \int_\Omega \int_{\mathbb{R}^{m\times n}} (W(F) + S(t_k) \cdot F)\nu_x(\mathrm{d}F) \, \mathrm{d}x + \sum_{i=1}^{M+1} \int_\Omega c^i |\lambda^i(x) - \lambda^i_{k-1}(x)| \, \mathrm{d}x$$

$$\text{subject to } (y, \nu, \lambda) \in \mathbb{P}' \ .$$

This problem is nonsmooth, so using the Mosco transform we define an equivalent smooth problem (with inequality constraints) which includes $M + 1$ auxiliary variables, namely

$$(30) \qquad \text{minimize } \int_\Omega \int_{\mathbb{R}^{m\times n}} (W(F) + S(t_k) \cdot F)\nu_x(\mathrm{d}F) \, \mathrm{d}x + \sum_{i=1}^{M+1} \int_\Omega a^i(x) \, \mathrm{d}x$$

$$\text{subject to } -a^i - c^i \mathcal{L}^i \bullet \nu \le -c^i \lambda^i_{k-1} \ \forall \ 1 \le i \le M+1$$

$$-a^i + c^i \mathcal{L}^i \bullet \nu \le c^i \lambda^i_{k-1} \ \forall \ 1 \le i \le M+1$$

$$(y, \nu, \lambda) \in \mathbb{P}' \ , a^i \in L^2(\Omega)$$

We invite the reader to verify that (29) and (30) are equivalent in the sense that minima are the same and if (y, ν, λ) solves (29) then $(y, \nu, \lambda, \{c|\lambda^i - \lambda^i_{k-1}|\}_i)$ solves (30) and conversely if $(y, \nu, \lambda, \{a^i\}_i)$ solves (30) then (y, ν, λ) solves (29). A proof can be also found in [17].

9

3. Optimality conditions for (30)

We are going to show that every solution to (30) sastisfies a maximum principle with the following Hamiltonian

$$(31) \quad \mathcal{H}_\mu(t, x, F) := -W(F) + S(t) \cdot F + \mu_0(x) \cdot \mathbb{T}(F) + \sum_{i=1}^{M+1} c^i(\mu_1^i(x) - \mu_2^i(x))\mathcal{L}^i(F) \, ,$$

where $\mu = (\mu_0, \mu_1^1, \mu_2^1, \ldots, \mu_1^{M+1}, \mu_2^{M+1})$ is a vector of Lagrange multipliers. Here μ_0 is the vector multiplier related to the constraint $\int_{\mathbb{R}^{m \times n}} \mathbb{T}(F)\nu_x(\mathrm{d}F) = \mathbb{T}(\nabla y(x))$, μ_1^i is a Lagrange multiplier to the constraint $-a^i/c^i - \mathcal{L}^i \bullet \nu \leq -\lambda_{k-1}^i$, while μ_2^i is a Lagrange multiplier to the constraint $-a^i/c + \mathcal{L}^i \bullet \nu \leq \lambda_{k-1}^i$ for $i = 1, \ldots, M + 1$. In particular, as we will see below, it must hold that $\mu_1^i + \mu_2^i = 1$ and both are nonnegative. Having the Hamiltonian, the following maximum principle holds.

Proposition 3.1. *If we solve (30) for $q \in \mathbb{P}'$ it holds for almost all $x \in \Omega$ that the ν-component of q satisfies*

$$(32) \qquad \max_{F \in \mathbb{R}^{m \times n}} \mathcal{H}_\mu(t_k, x, F) = \int_{\mathbb{R}^{m \times n}} \mathcal{H}_\mu(t_k, x, s)\nu_x(\mathrm{d}s) \, .$$

Remark 3.2. *If there is no dissipation, i.e., $\mathcal{L} = 0$, and no loading, i.e., $S = 0$, the Hamiltonian in (31) is the same as in [8].*

The maximum principle encodes the first-order optimality conditions which are only necessary because the problem (30) is nonconvex. Indeeed, it is due to the constraint

$$(33) \qquad \int_{\mathbb{R}^{m \times n}} \mathbb{T}(F)\nu_x(\mathrm{d}F) = \mathbb{T}(\nabla y(x))$$

imposed for almost all $x \in \Omega$ and all admissible Young measures and deformations. Nevertheless, fixing $x \in \Omega$, (33) is linear. Thus, we may distinguish two different scales in (30). On a large scale, we minimize over the admissible deformation $y \in \mathbb{Y}^p(\Omega; \mathbb{R}^m)$ and on a smaller scale, having y fixed, we look for an optimal Young measure. This is already a convex problem. Then the optimality conditions (32) are not only necessary but also sufficient.

Therefore, let us now consider the situation that we want to solve (30) but we look for the solution only among homogeneous (i.e. independent of x) elements from $\mathbb{P}'$ with a given first moment, say $A \in \mathbb{R}^{m \times n}$, i.e., $\bar{\nu} := \int_{\mathbb{R}^{m \times n}} F\nu(\mathrm{d}F) = A$. Finally, we suppose that λ_{k-1} also does not depend on x and that the loading S is fixed. Altogether, we consider the following problem: given $\lambda_{k-1}^i \in \mathbb{R}$ for all $1 \leq i \leq M + 1$ solve

$$
\text{(34)} \qquad \text{minimize} \int_{\mathbb{R}^{m\times n}} (W(F) - S \cdot F)\nu(\mathrm{d}F) + \sum_{i=1}^{M+1} a^i
$$

$$
\text{subject to } -a^i - c^i \mathcal{L}^i \bullet \nu \le -c^i \lambda_{k-1}^i \ \forall \ 1 \le i \le M+1
$$

$$
-a^i + c^i \mathcal{L}^i \bullet \nu \le c^i \lambda_{k-1}^i \ \forall \ 1 \le i \le M+1
$$

$$
\nu \in \mathbb{P}'_{\mathrm{hom}} \ , \ \bar{\nu} = A \ , \ a^i \ge 0 \ ,
$$

where $\mathbb{P}'_{\mathrm{hom}}$ stands for homogeneous (i.e. independent of $x \in \Omega$) measures from $\mathbb{P}'$. This problem is convex and therefore the maximum principle stated in Proposition 32 forms necessary but also sufficient conditions for a minimizer to (34).

In particular, having a solution to the problem (34) we also know the values of Lagrange multipliers μ, say μ^*. Then the solution to (34) is the same as the solution to the following minimization problem:

$$
\text{(35)} \qquad \text{minimize} \int_{\mathbb{R}^{m\times n}} \left(W(F) - S \cdot F - \mu_0^* \cdot \mathbb{T}(F) + \sum_{i=1}^{M+1} (\mu_2^{i*} - \mu_1^{i*})\mathcal{L}^i(F) \right) \nu(\mathrm{d}F)
$$

$$
\text{subject to } \nu \in \mathbb{P}'_{\mathrm{hom}} \ , \ \bar{\nu} = A \ .
$$

In each time step, (35) is a smooth convex minimization problem. The optimal value of the objective function is the polyconvex envelope of $F \mapsto W(F) - S \cdot F - \mu_0^* \cdot \mathbb{T}(F) + \sum_{i=1}^{M+1}(\mu_2^{i*} - \mu_1^{i*})\mathcal{L}^i(F)$ evaluated at the point $A \in \mathbb{R}^{m\times n}$.

Remark 3.3. *Problem (30) is an example of a Stackelberg leadership game. The deformation y is a leader while particular probability measures ν_x, $x \in \Omega$, are followers trying to minimize the energy if y is fixed. Thus, (35) is just a single follower problem where the follower is the Young measure minimizing the objective function keeping the first moment of the Young measure fixed.*

In order to derive optimality conditions for (34) we consider the functional $\Phi : \mathbb{P}'_{\mathrm{hom}} \times \mathbb{R}^{M+1} \to \mathbb{R}$ defined by

$$
\text{(36)} \qquad \Phi(\nu, a) := \int_{\mathbb{R}^{m\times n}} (W(F) - S \cdot F)\nu(\mathrm{d}F) + \sum_{i=1}^{M+1} a^i \ .
$$

Moreover, set $\Pi(\nu, a) = \mathbb{T} \bullet \nu - \mathbb{T}(A)$, where $\Pi : \mathbb{P}'_{\mathrm{hom}} \times \mathbb{R}^{M+1} \to \mathbb{R}$. To treat the inequality constraint in (34) we define for $i \in \{1, \dots, M+1\}$

$$
R_1^i(\nu, a) = -a^i - c^i \mathcal{L}^i \bullet \nu
$$

and

$$
R_2^i(\nu, a) = -a^i + c^i \mathcal{L}^i \bullet \nu \ ,
$$

where $R_i^j : \mathbb{P}'_{\mathrm{hom}} \times \mathbb{R}^{M+1} \to \mathbb{R}$ for $j = 1, \dots, M+1$.

Finally, (34) can be reformulated as follows

(37)
$$\left.\begin{array}{ll}\text{minimize} & \Phi(\nu, a) \\ \text{subject to} & \Pi(\nu, a) = 0 \\ & R_1^i(\nu, a) \leq -c^i \mathcal{L}^i \bullet \nu_{k-1} \\ & R_2^i(\nu, a) \leq c^i \mathcal{L}^i \bullet \nu_{k-1} \\ & (\nu, a) \in \mathbb{P}'_{\text{hom}} \times \mathbb{R}^{M+1} \ . \end{array}\right\}$$

Note that Π, R_1^i and R_2^i are continuous and linear. Let us still denote $\mathbb{M}_1^i = \{f \in \mathbb{R}; f \leq -c^i \mathcal{L}^i \bullet \nu_{k-1}\}$ and $\mathbb{M}_2^i = \{f \in \mathbb{R}; f \leq c^i \mathcal{L}^i \bullet \nu_{k-1}\}$ and we write for $j = 1, 2$

$$(R_i^j)^{-1}(\mathbb{M}_i^j) = \{(\nu, a) \in \mathbb{P}'_{\text{hom}} \times \mathbb{R}; \ R_i^j(\nu, a) \in \mathbb{M}_i^j\} \ .$$

The optimality conditions states ([2, p. 174, Th. 16]) that if (ν, a) is a solution then

(38)
$$\begin{aligned} \nabla \Phi(\nu, a) \ \in \ & -N_{\text{Ker}\Pi \cap (R_1^i)^{-1}(\mathbb{M}_1^i) \cap (R_2^i)^{-1}(\mathbb{M}_2^i) \cap (\mathbb{P}'_{\text{hom}} \times \mathbb{R}^{M+1})}(\nu, a) \\ = \ & \text{Range} \ \Pi^* - [R_1^i]^* N_{\mathbb{M}_1^i}(R_1^i(\nu, a)) - [R_2^i]^* N_{\mathbb{M}_2^i}(R_2^i(\nu, a)) \\ & - N_{\mathbb{P}'_{\text{hom}} \times \mathbb{R}^{M+1}}(\nu, a) \\ = \ & \text{Range} \ \Pi^* - [R_1^i]^* N_{\mathbb{M}_1^i}(R_1^i(\nu, a)) - [R_2^i]^* N_{\mathbb{M}_2^i}(R_2^i(\nu, a)) \\ & - N_{\mathbb{P}'_{\text{hom}}}(\nu) \times \{0\} \ . \end{aligned}$$

This means that there exist Lagrange multipliers $\mu^0 \in \mathbb{R}^\sigma$, $\mu_1^i \in N_{\mathbb{M}_1^i}(R_1^i(\nu, a))$, $\mu_2^i \in N_{\mathbb{M}_2^i}(R_2^i(\nu, a))$ such that for $1 \leq i \leq M+1$

(39)
$$\Pi_{a^i}^* \mu - [R_1^i(\nu, a)]_{a^i}^* \mu_1^i - [R_2^i(\nu, a)]_{a^i}^* \mu_2 - \nabla_{a^i} \Phi(\nu, a) = 0 \ ,$$

(40)
$$\Pi_\nu^* \mu - [R_1^i(\nu, a)]_\nu^* \mu_1 - [R_2^i(\nu, a)]_\nu^* \mu_2 - \nabla_\nu \Phi(\nu, a) \in N_{\mathbb{P}'_{\text{hom}}}(\nu) \ ,$$

where $N_{\mathbb{P}'_{\text{hom}}}(\nu)$ denotes the normal cone to $\mathbb{P}'_{\text{hom}}$ at the point $\nu \in \mathbb{P}'_{\text{hom}}$, i.e.,

$$N_{\mathbb{P}'_{\text{hom}}}(\nu) := \{\xi \in C_0(\mathbb{R}^{m \times n})^{**}; \ \forall \tilde{\nu} \in \mathbb{P}'_{\text{hom}} \ \langle \xi, \tilde{\nu} \rangle \leq \langle \xi, \nu \rangle\} \ .$$

We start with a computation of $\nabla \Phi$.

Lemma 3.4. *Let $W : \mathbb{R}^{m \times n} \to \mathbb{R}$ be continuous and let $a \in \mathbb{R}^{M+1}$. Then it holds that $\nabla \Phi(\nu, a) = (W - S, 1, \dots, 1)$.*

Proof. It is easy because Φ depends on (ν, a) linearly. □

Lemma 3.5. *It holds $\Pi^* \mu = (\mu_0 \mathbb{T} - \mu_0 \mathbb{T}(A), 0)$ for any $\mu \in \mathbb{R}^\sigma \times \mathbb{R}^{M+1}$.*

Proof. We have

$$\langle \Pi^* \mu, (\nu, a) \rangle \quad = \quad \langle \mu, \Pi(\nu, a) \rangle = \langle \mu, \mathbb{T} \bullet \nu - \mathbb{T}(A) \rangle = \langle \nu, \mu_0 \mathbb{T} - \mu_0 \mathbb{T}(A) \rangle \ .$$

$\square$

Lemma 3.6. *It holds* $[R_1^i]^* \mu_1^i = (-\mu_1^i c^i \mathcal{L}^i, -\mu_1^i)$ *and* $[R_2^i]^* \mu_2^i = (\mu_2^i c^i \mathcal{L}^i, -\mu_2^i)$ *for any* $\mu_1^i, \mu_2^i \in \mathbb{R}$.

Proof. We compute only the expression for $R^1 \mu_1$ as the other can be obtained similarly. We have

$$\langle [R_i^1]^* \mu_1^i], (\nu, a) \rangle = \langle \mu_1^i, R_1^i(\nu, a) \rangle = \langle \mu_1^i, -a^i - c^i \mathcal{L}^i \bullet \nu \rangle = -\langle \nu, c^i \mu_1^i \mathcal{L}^i \rangle - \langle \mu_1^i, a^i \rangle \ .$$

$\square$

Gathering now all the results from Lemmata 3.4-3.6 we get that (39-40) say that if $(\nu, a) \in \mathbb{P}'_{\text{hom}} \times \mathbb{R}^{M+1}$ solve (37) then there are $\mu_0 \in N_{\text{Ker}\Pi}(\nu, a)$ and $\mu_1^i \in N_{\mathbb{M}_1^i}(R_1^i(\nu, a))$ for $1 \le i \le M + 1$

$$(41) \qquad -W + S \cdot + \mu(\mathbb{T} - \mathbb{T}(A)) + (\mu_1^i - \mu_2^i) c^i \mathcal{L}^i \in N_{\mathbb{P}'_{\text{hom}}}(\nu) \ ,$$

$$(42) \qquad \qquad 1 = \mu_1^i + \mu_2^i \ .$$

As $\nabla_\nu \Phi$ as well as Π_ν^* and $R_j^i \nu$ (for $j = 1, 2$) take their values in $C_p(\mathbb{R}^{m \times n})$ rather than in $C_0(\mathbb{R}^{m \times n})^{**}$ we can study only the intersection of the normal cone $N_{\mathbb{P}'_{\text{hom}}}(\nu)$ with $C_p(\mathbb{R}^{m \times n})$. Hence,

$$(43) \qquad N_{\mathbb{P}'_{\text{hom}}}(\nu) \cap C_p(\mathbb{R}^{m \times n}) = \{ h \in C_p(\mathbb{R}^{m \times n}); \ \forall \tilde{\nu} \in \mathbb{P}'_{\text{hom}} \langle \tilde{\nu}, h \rangle \le \langle \nu, h \rangle \}$$

$$= \left\{ h \in C_p(\mathbb{R}^{m \times n}); \ \langle \nu, h \rangle = \sup_{\tilde{\nu} \in \mathbb{P}'_{\text{hom}}} \langle \tilde{\nu}, h \rangle = \sup_{F \in \mathbb{R}^{m \times n}} h(F) < +\infty \right\} \ ,$$

Now we are ready to formulate the maximum principle for the Hamiltonian $\mathcal{H}_{\mu, \mu_1, \mu_2} \in C_p(\mathbb{R}^{m \times n})$ given here by (we drop dependence on x, t for simplicity)

$$(44) \qquad \mathcal{H}_\mu(F) := -W(F) + S \cdot s + \mu \cdot \mathbb{T}(F) + \sum_{i=1}^{M+1} c^i(\mu_1^i - \mu_2^i) \mathcal{L}^i(F) \ .$$

Proposition 3.7. *Let* $S \in \mathbb{R}^{m \times n}$ *and let* $p > \min(m, n)$. *Let* $(\nu, a) \in \mathbb{P}'_{\text{hom}} \times \mathbb{R}^{M+1}$ *solve* (37). *Then there are nonnegative* $\mu_1^i, \mu_2^i \in [0, 1]$ *and* $\mu_0 \in \mathbb{R}^\sigma$ *such that*

$$(45) \qquad \langle \nu, \mathcal{H}_\mu \rangle = \sup_{F \in \mathbb{R}^{m \times n}} \mathcal{H}_\mu(F)$$

$$(46) \qquad \qquad 1 = \mu_1^i + \mu_2^i \ ,$$

$$(47) \qquad \qquad \langle \nu, \mathbb{T} \rangle = T(A) \ ,$$

13

$$(48) \qquad\qquad \mu_1^i R_1^i(\nu, a) = \mu_1^i c^i \mathcal{L}^i \bullet \nu_{k-1} \ ,$$

$$(49) \qquad\qquad \mu_2^i, R_2^i(\nu, a) = \mu_2^i c^i \mathcal{L}^i \bullet \nu_{k-1} \ .$$

Conversely, if $(\nu, a) \in \mathbb{P}'_{\text{hom}} \times \mathbb{R}^{M+1}$, $\Pi(\nu, a) = 0$, $R_1^i(\nu, a) \leq -c^i \mathcal{L}^i \bullet \nu^{k-1}$, $R_2^i(\nu, a) \leq c^i \mathcal{L}^i \bullet \nu^{k-1}$, $1 \leq i \leq M+1$ *and (39-49) hold for some nonnegative* μ_1, μ_2 *then* (ν, a) *solve* (37).

Proof. The necessity follows from (43) and from the optimality conditions above and sufficiency follows from the convexity of (37). The fact that μ_j^i, $j = 1, 2$, satisfies (48) and (49), respectively, follows from the definition of the normal cone; cf. [12]. Notice that $\mu_1^i - \mu_2^i$ belong to the subdifferential of $|\cdot|$ for all i, i.e., $\mu_1^i - \mu_2^i \in [-1, 1]$. This together with (46) shows nonnegativity of μ_j^i.

$\square$

In case of an inhomogeneous problem (30) the Hamiltonian of the problem is x-dependent and given by (31). Indeed, fixing a minimizing deformation $y \in \mathbb{Y}$ the Young measure $\{\nu_x\}_{x \in \Omega}$ is optimizes the energy on the microscale solving in each time step (34) for $A := \nabla y(x)$. In what follows, we show how to use advantageously the the maximum principle in a numerical-solution strategy. This approach was first suggested and tested in a static scalar one-dimensional example in [9] and further used in micromagnetics calculations in [17, 19].

4. Numerical approximations

We are about to discuss spatial discretization of incremental problems (23) and discribe an efficient strategy leading to their solutions. In order to keep the explanation as simple as possible, we confine ourselves to the case of two wells, i.e., $M = 1$ and instead of surface forces we drive the evolution of our specimen by time-dependent boundary conditions, i.e., we set $S = 0$. It is straightforward to generalize the method to a more general scenario.

4.1. **Problem description.** Recall that the volume fraction is defined by

$$\lambda(x) = \int_{\mathbb{R}^{m \times n}} \mathcal{L}(F) \nu_x(\mathrm{d}F)$$

for almost every $x \in \Omega$. We have by the definition of $\mathcal{L}$ that $\sum_{j=0}^{M} \lambda^j = \sum_{j=0}^{M} \mathcal{L}^j = 1$. Therefore, if $M = 1$, i.e., in case of the so-called double-well problem we have that $\lambda^2 := 1 - \lambda^1$. Thus, having two pairs $(\lambda_1, 1 - \lambda_1)$ and $(\lambda_2, 1 - \lambda_2)$ we have by (10) that $\mathcal{D}(q_1, q_2) := \int_\Omega (c^1 + c^2) |\lambda^1 - \lambda^2| \, \mathrm{d}x$. In order to simplify the notation, we set $c_\mathcal{D} := c^1 + c^2$. The dissipation functional then reads

$$\mathcal{D}(q_1, q_2) = c_\mathcal{D} \int_\Omega |\lambda^1 - \lambda^2| \mathrm{d}x,$$

4.2. General discrete problem. Given a finite element partition $\mathcal{T}$ of Ω with $\mathrm{diam}(T) \leq h$ for all $T \in \mathcal{T}$ and a set $\mathcal{A}_{d,r} \subset \mathbb{R}^{m \times n}$ we consider a Young measure $\nu = \{\nu_x\}_{x \in \Omega}$ where $\nu_x|_T := \sum_{A \in \mathcal{A}_{d,r}} \theta_{T,A} \delta_A$, with $\{\theta_{T,A}\}_{A \in \mathcal{A}_{d,r}}$ coefficients of a convex combination, and δ_A the Dirac mass supported at A. The deformation y is approximated by a continuous, element-wise affine map y_h defined by its nodal values at the set of nods $\mathcal{N}_h$. A typical time step t_j of the discrete version of (30) consists in solving the following optimization problem:

Find $\left((y_h(z))_{z \in \mathcal{N}_h}, (a_h|_T)_{T \in \mathcal{T}}, (\theta_{T,A})_{T \in \mathcal{T}, A \in \mathcal{A}_{d,r}}\right)$ which minimizes

$$\sum_{T \in \mathcal{T}} |T| \sum_{A \in \mathcal{A}_{d,r}} \theta_{T,A} W(A) + \sum_{T \in \mathcal{T}} c_{\mathcal{D}} |T| a_h|_T$$

subject to $\quad y_h|_{\Gamma_D} = y_{D,h}(t_j, \cdot), \; \theta_{T,A} \geq 0, \; \sum_{A \in \mathcal{A}_{d,r}} \theta_{T,A} = 1, \; a_h|_T \geq 0 \quad$ and

$$\mathbb{T}(\nabla y_h|_T) = \sum_{A \in \mathcal{A}_{d,r}} \theta_{T,A} \mathbb{T}(A),$$

$$- a_h|_T / c_{\mathcal{D}} - \sum_{A \in \mathcal{A}_{d,r}} \theta_{T,A} \mathcal{L}^1(A) \leq -\lambda^1_{h,j-1}|_T,$$

$$- a_h|_T / c_{\mathcal{D}} + \sum_{A \in \mathcal{A}_{d,r}} \theta_{T,A} \mathcal{L}^1(A) \leq \lambda^1_{h,j-1}|_T,$$

for all $T \in \mathcal{T}$.

Notice that the constraint with the left-hand side $\mathbb{T}(\nabla y_h|_T)$ is nonlinear if $\min(m,n) \geq 2$. Otherwise, this defines a linear program which we solve iteratively with an active set strategy based on the maximum principle of Section 3. Given the (approximate) solution of this problem, the next time step t_{j+1} is the same problem with $y_{D,h}(t_j)$ replaced by $y_{D,h}(t_{j+1})$ and $\lambda_{h,j-1}$ replaced by

$$\lambda^1_{h,j}|_T = c_{\mathcal{D}} \sum_{A \in \mathcal{A}_{d,r}} \theta_{T,A} \mathcal{L}^1(A)$$

for all $T \in \mathcal{T}$.

4.3. Simplification through enforced homogeneity. In order to simplify the calculations we consider solutions of the model problem which are spatially homogeneous and the deformation is entirely defined through the affine boundary data $F_D(t)$, i.e., the deformation $y(t, x) = F_D(t)x$ for all $x \in \Omega$ is fully prescribed in the entire evolution. Hence the minimization problem in the j-th time step reduces to:

minimize $\quad \displaystyle\int_{\mathbb{R}^{m \times n}} W(F) \nu(\mathrm{d}F) + c_{\mathcal{D}} a \quad$ among $(a, \nu) \in \mathbb{R} \times \mathbb{P}'_{\mathrm{hom}}$

subject to $\quad a \geq 0 \quad \displaystyle\int_{\mathbb{R}^{m \times n}} F \nu(\mathrm{d}F) = F_D(t_j)$

$$- a/c_{\mathcal{D}} - \int_{\mathbb{R}^{m \times n}} \mathcal{L}^1(F) \nu(\mathrm{d}F) \leq -\lambda^1_{j-1}, \quad -a/c_{\mathcal{D}} + \int_{\mathbb{R}^{m \times n}} \mathcal{L}^1(F) \nu(\mathrm{d}F) \leq \lambda^1_{j-1}.$$

4.4. Discretization of spatially homogeneous problems.

We choose a finite subset $\mathcal{A}_{d,r} \subset \mathbb{R}^{m \times n}$ and discretize the convex set of (homogeneous) Young measures by

$$\mathbb{P}'_{\text{hom}} \supset YM^{hom}_{\mathcal{A}_{d,r}} = \Big\{ \nu_{d,r} = \sum_{A \in \mathcal{A}_{d,r}} \theta_A \delta_A : \theta_A \geq 0, \sum_{A \in \mathcal{A}_{d,r}} \theta_A = 1 \Big\}.$$

Typically, $\mathcal{A}_{d,r}$ will be a subset of $d\mathbb{Z}^{n \times n} \cap B^\infty_r(0)$. We will identify a discrete Young measure with its convex coefficients $\theta = (\theta_A)_{A \in \mathcal{A}_{d,r}}$. This choice leads to the following discretization of the homogeneous vecotorial problem described above:

$$\text{minimize} \quad \sum_{A \in \mathcal{A}_{d,r}} \theta_A W(A) + c_{\mathcal{D}} a \quad \text{among } (a, \nu_{d,r}) \in \mathbb{R} \times YM^{hom}_{\mathcal{A}_{d,r}}$$

$$\text{subject to} \quad \sum_{A \in \mathcal{A}_{d,r}} \theta_A A = F_{\mathrm{D}}(t_j), \quad \mathbb{T}(F_{\mathrm{D}}(t)) = \sum_{A \in \mathcal{A}_{d,r}} \theta_A \mathbb{T}(A),$$

$$a \geq 0, \quad -a/c_{\mathcal{D}} - \sum_{A \in \mathcal{A}_{d,r}} \theta_A \mathcal{L}^1(A) \leq -\lambda^1_{j-1}, \quad -a/c_{\mathcal{D}} + \sum_{A \in \mathcal{A}_{d,r}} \theta_A \mathcal{L}^1(A) \leq \lambda^1_{j-1}.$$

We subsequently set $\lambda^1_j = \sum_{A \in \mathcal{A}_{d,r}} \theta_A \mathcal{L}^1(A)$.

4.5. Efficient solution via active set strategy.

The discrete problem is a linear optimization problem which can be solved directly with standard algorithms. Realizing that only a small number of coefficients θ_A will be non-vanishing, it is desirable to employ an iterative scheme in which a large number of vanishing or small coefficients will not be incorporated in the approximating problems. The key to such an iterative method is the optimality condition

$$\max_{A \in \mathcal{A}_{d,r}} \big(\mathbb{T}(A) \cdot \mu_0 - W(A) + c_{\mathcal{D}}(\mu^1 - \mu^2)\mathcal{L}^1(A) \big)$$

$$= \sum_{A \in \mathcal{A}_{d,r}} \big(\theta_A \mathbb{T}(A) \cdot \mu^0 - W(A) + c_{\mathcal{D}}(\mu^1 - \mu^2)\mathcal{L}^1(A) \big),$$

where μ_0 is the Lagrange multiplier related to the equality constraints involving $F_{\mathrm{D}}(t_j)$ and $\mathbb{T}(F_{\mathrm{D}}(t_j))$ and (μ_1, μ_2) are the multipliers related to the inequality constraints involving a. Notice that we write μ_1, μ_2 instead of μ^1_1 and μ^1_2 to simplify the notation. It shows that only those atoms $A \in \mathcal{A}_{d,r}$ can have a convex coefficient θ_A different from zero, for which the function on the left-hand side assumes its maximum. Given a guess or a good approximation of the Lagrange multipliers and some tolerance $\varepsilon > 0$, those atoms A are activated within an iterative strategy for which the maximum is attained up to the tolerance ε. This defines the set new set $\mathcal{A}_{d,r}$. If the solution of the (reduced) linear program satisfies the maximum principle (up to a small tolerance chosen equal to the grid size d) for the full set of atoms then the solution is accepted and otherwise the activation parameter is enlarged and a new (presumably larger) active set is computed based on the new approximate multipliers. Since the optimality conditions are necessary and sufficient the iterative strategy converges. To obtain accurate initial guesses, this strategy is combined with a multilevel scheme in which the discretization parameter d is gradually decreased. In our implementation the (reduced) optimization problems were

solved with the Matlab routine `linprog`. The precise scheme for the solution of one time step reads as follows.

Algorithm ($A^{hom}_{active\ set}$). Input: Parameters $0 < d_{final} \leq r$, number of levels $J \geq 0$ such that $2^J d_{final} \leq r$, time step t_j, vector $\lambda_{j-1} \in \mathbb{R}^{M+1}$.

(1) Set $d = 2^J d_{final}$, $\mu_0 = 0$, $\mu_1 = 0$, $\mu_2 = 0$, and $\varepsilon_{mp} = d/2$.
(2) Define
$$\mathcal{A}_{d,r} = \Big\{ A \in d\mathbb{Z}^{n \times n} \cap B_r^\infty(0) : \mathcal{H}_\mu(t_j, A) \geq \sum_{B \in \mathcal{A}_{d,r}} \theta_B \mathcal{H}_\mu(t_j, B) - \varepsilon_{mp} \Big\},$$
where $\mathcal{H}_\mu(t_j, A) = \mathbb{T}(A) \cdot \mu_0(t_j) - W(A) + c_\mathcal{D}(\mu_1(t_j) - \mu_2(t_j)) \cdot \mathcal{L}^1(A)$.
(3) Add further elements $A \in \mathbb{R}^{m \times n}$ to ensure feasibility and solve the linear program described in Section 4.4 with the set $\mathcal{A}_{d,r}$. This provides updates of the multipliers μ_0, μ_1, μ_2.
(4) If there exists $A \in d\mathbb{Z}^{n \times n} \cap B_r^\infty(0)$ with
$$\mathcal{H}_\mu(t_j, A) > \sum_{B \in \mathcal{A}_{d,r}} \theta_B \mathcal{H}_\mu(t_j, B)$$
then set $\varepsilon_{mp} = 2\varepsilon_{mp}$ and go to (2).
(5) If $d > d_{final}$ set $d = d/2$ and $\varepsilon_{mp} = d/2$ and go to (2).

We consider the following specification of the model problem:

Example 4.1. *Let $m = n = 2$, $\mathfrak{T} = 1$, $\lambda_0 = 0$,*
$$W(F) = \min\big\{ |F^T F - F_1^T F_1|^2/2, |F^T F - F_2^T F_2|^2/2 \big\}$$
for $F_1 = \mathrm{diag}(\delta, 1/\delta)$, $F_2 = \mathrm{diag}(1/\delta, \delta)$, and $F(t) = (1-t)F_1 + tF_2$. The function $\mathcal{L}^1$ is for given $\epsilon > 0$ chosen as
$$\mathcal{L}^1(F) = f_C\big([F^T F]_{11}\big)$$
with
$$f_C(z) = \begin{cases} 0 & z \geq \delta^2 - \epsilon \\ (z - (\delta^2 - \epsilon F))/(1/\delta^2 + 2\epsilon - \delta^2) & 1/\delta^2 + \epsilon \leq z \leq \delta^2 - \epsilon \\ 1 & z \leq 1/\delta^2 + \epsilon \end{cases}$$
The value of ϵ relates to the elastic region of the material. Indeed, starting the evolution with the Young measure supported in one of the energy wells of W, the parameter ϵ determines "how far" the support can move without any dissipation. For the experiments we choose $\epsilon = 1/20$ and $\delta = \sqrt{5/4}$.

We employed $d = 1/20$, $\tau = 1/40$, $r = 2$, and
$$c_\mathcal{D} = 1, 1/10, 1/100$$
in our experiments. The multilevel strategy always started with the coarse grid defined by $d = 1$. In Figure 1 we displayed for the time steps $t_j = j/40$ for $j = 0, 10, 20, 30, 40$ (form left to right) and the dissipation coefficients $c_\mathcal{D} = 1, 1/10,$ and $1/100$ (from
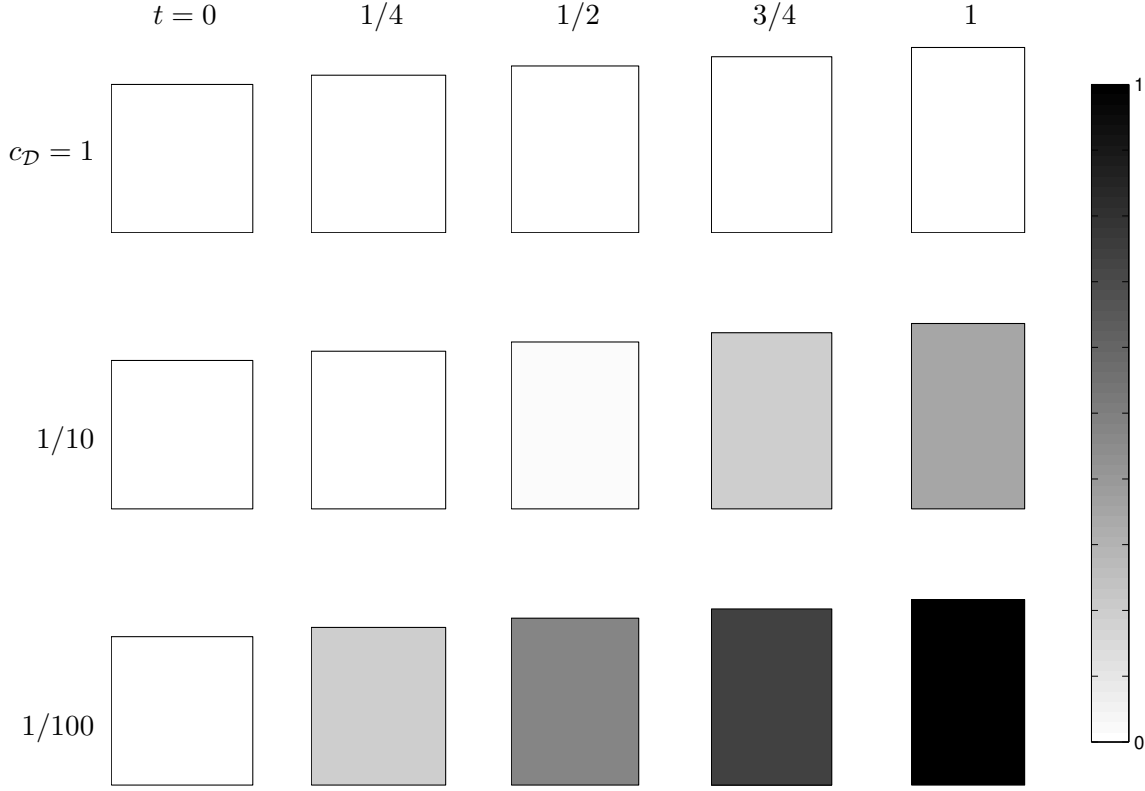
17

FIGURE 1. Transformation of a specimen for different dissipation strengths. The upper row shows the deformed body colored by the volume fraction $\lambda^1(t_j)$ for $t_j = j/40$, $j = 0, 10, 20, 30, 40$, and $c_{\mathcal{D}} = 1$. The second and third row show the related quantities for $c_{\mathcal{D}} = 1/10$ and $c_{\mathcal{D}} = 1/100$, respectively.

top to bottom) the deformed body $F_{\mathrm{D}}(t)\Omega$ for $\Omega = (0,1)^2$ and, indicated by the gray shading, the volume fraction λ^1_j. We see that the specimen does not transform for the large dissipation constant but does for the other values of $c_{\mathcal{D}}$. This is what we observe in physical experiments because large dissipation, i.e., large $c_{\mathcal{D}}$ makes the transformation more difficult, or not possible at all.

In Figure 2 we plotted the functions

$$t_j \mapsto W\big(F_{\mathrm{D}}(t_j)\big),$$
$$t_j \mapsto I(t_j) = \sum_{A \in d\mathbb{Z}^{2\times 2}} \theta^j_A W(A) + c_{\mathcal{D}} a,$$
$$t_j \mapsto \mathcal{D}(\delta q_j) = c_{\mathcal{D}} a_j = c_{\mathcal{D}} |\lambda_j - \lambda_{j-1}|, \quad \lambda^1_j = \sum_{A \in \mathcal{A}_{d,r}} \theta_{A,j} \mathcal{L}^1(A)$$

for $c_{\mathcal{D}} = 1$, $1/10$, and $1/100$.

For $c_{\mathcal{D}} = 1/100$ we plotted in Figure 3 the relative number of activated atoms on the finest level corresponding to $d = 1/10$ for each time step. Notice that we have here for
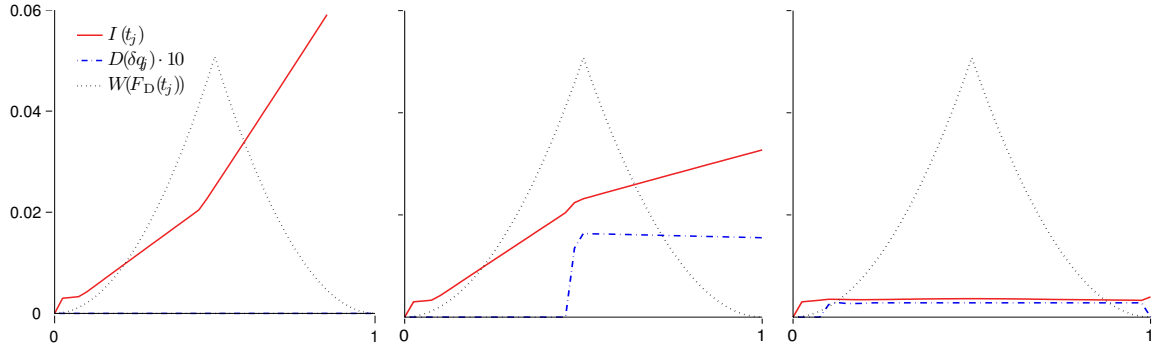
FIGURE 2. Total energy, dissipation, elastic energy, and elastic energy for the macroscopic deformation for $c_{\mathcal{D}} = 1$, $1/10$, and $1/100$ (from left to right).
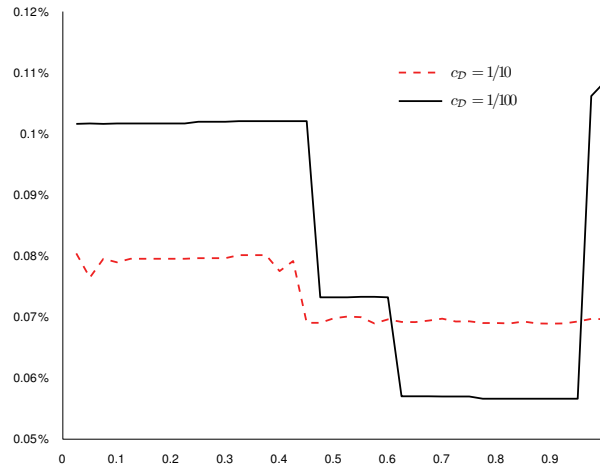

FIGURE 3. Relative number of activated atoms during the evolution for different dissipation constants.

$d = 1/10$ and $r = 2$

$$\operatorname{card}\left(d\mathbb{Z}^{2\times 2} \cap B_r^\infty(0)\right) = 2\,825\,761.$$

We thus obtain an average reduction to about 0.1% of the theoretical number of atoms. We remark that for $c_{\mathcal{D}} = 1$ we obtained different results.

4.6. **Scalar experiment with spatial dependence.** We consider the following specification of the model problem:

Example 4.2. *Let $\Omega = (0,1)^2$, $\mathfrak{T} = 1$, $\Gamma_{\mathrm{D}} = \partial\Omega$, $u_D(x,t) = \sin(2\pi t)x_1$, $\lambda_0(x) = 1/2$,*

$$W(F) = \min\left\{|F - F_1|^2/2 + c_1, |F - F_2|^2/2 + c_2\right\}$$

for $F_1 = (1,0)^T$, $F_2 = (-1,0)^T$, $c_1 = 1/5$, and $c_2 = 0$.

19

For a triangulation of Ω consisting of 32 triangles, the set $\mathcal{A}_{d,r}$ defined through $d = 2^{-4}$ and $r = 2$, the time-step size $\tau = 1/80$, and the choices of constants

$$c_{\mathcal{D}} = 1 \quad \text{and} \quad c_{\mathcal{D}} = 1/10$$

Figures 4 and 5, respectively, show snapshots of the evolution for $t = j/20$ with $j = 1, 5, 10, 20$.

Figure 6 displays the energy and the dissipation contribution, i.e., the quantities

$$E(t_j) = \int_\Omega \int_{\mathbb{R}^2} W(A)\nu_{j,d,h}(\mathrm{d}A) + D(t_j)$$

$$= \sum_{T \in \mathcal{T}} |T| \sum_{A \in \mathcal{A}_{d,r}} \theta_{T,A}^j W(A) + D(t_j), \qquad D(t_j) = c_{\mathcal{D}} \int_\Omega a_{h,j}\,\mathrm{d}x = \sum_{T \in \mathcal{T}} |T| a_T(t_j)$$

as functions of $t \in [0,1]$ for $c_{\mathcal{D}} = 1$ and $c_{\mathcal{D}} = 1/10$.

Figure 6 illustrates hysteresis effects that occur in the evolution defined by the rate-independent process. We displayed the spatial averages of the (spatially constant) quantities $\partial_1 y_{h,j}$ and $\sigma_{h,j} \cdot \varrho$ on Γ_D, where

$$\sigma_{h,j} = \sum_{A \in \mathcal{A}_{d,r}} \theta_{A,j} DW(A).$$

The validity of a fully discrete analogue of the semi-discrete two-sided energy estimate (26):

$$m(t_j) := \int_{\Gamma_D} \sigma_{h,j} \cdot \varrho(u_{D,j} - u_{D,j-1})\,\mathrm{d}s$$

$$\leq \Xi(t_j) := \int_\Omega \int_{\mathbb{R}^2} W(s)\,\nu_{j,x}(\mathrm{d}s)\,\mathrm{d}x + c_{\mathcal{D}} \int_\Omega |\lambda_j^1 - \lambda_{j-1}^1|\,\mathrm{d}x - \int_\Omega \int_{\mathbb{R}^2} W(s)\,\nu_{j,x}(\mathrm{d}s)\,\mathrm{d}x$$

$$\leq \int_{\Gamma_D} \sigma_{h,j-1} \cdot \varrho(u_{D,j} - u_{D,j-1})\,\mathrm{d}s =: M(t_j)$$

is graphically analysed in Figure 7.

4.6.1. *Scalar, inhomogeneous example.* We consider the following specification of the model problem which leads to an inhomogeneous solution:

Example 4.3. *Let $n = 2$, $m = 1$, $\Omega = (0,1)^2$, $\mathfrak{T} = 1$, $\Gamma_D = \partial\Omega$, $\lambda_0(x) = 1/2$, and the displacement*

$$u_D(t,x) = \begin{cases} -3(z - z_b)^5/128 - (z - z_b)^3/3 & \text{for } z \leq x_b \\ (z - z_b)^3/24 + (z - z_b) & \text{for } z \geq x_b \end{cases}$$

for $z = x \cdot F_0$, $z_b = 1/2$, $F_0 = (\cos\phi, \sin\phi)$, $\phi = \pi/6$, and

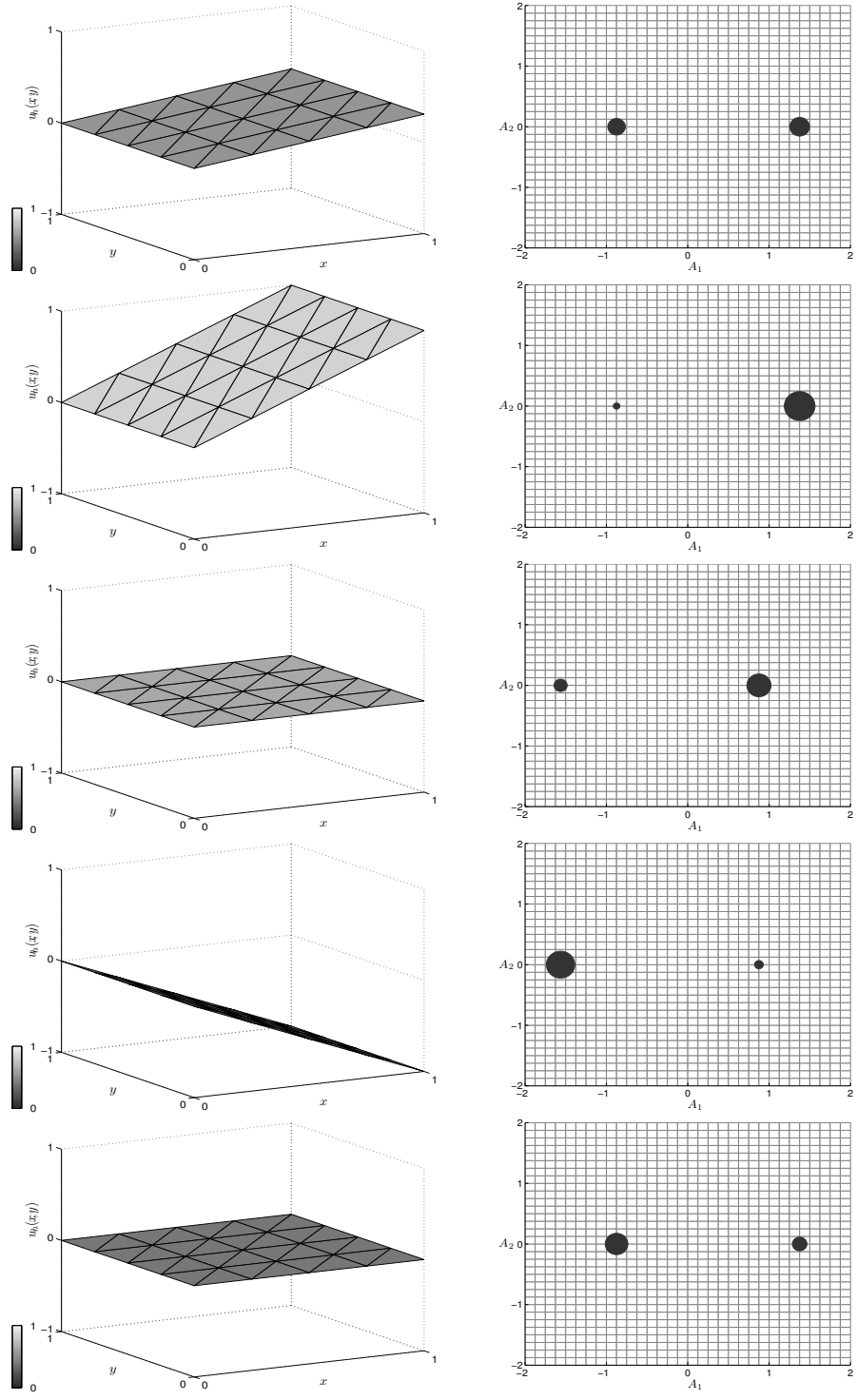$$W(F) = |F - F_0|^2 |F + F_0|^2.$$

20

FIGURE 4. Scalar displacement $u_{h,j}$ (left) and discrete Young measure $\nu_{j,h}$ (right) for $j = 4, 20, 40, 60, 80$ in Example 4.1 with $c_{\mathcal{D}} = 1$. The displacement is coloured by the quantity λ_h and the sizes of the dots in the grid in the right plots are proportional to the volume fraction associated to a grid point. The grid indicates every second atom.
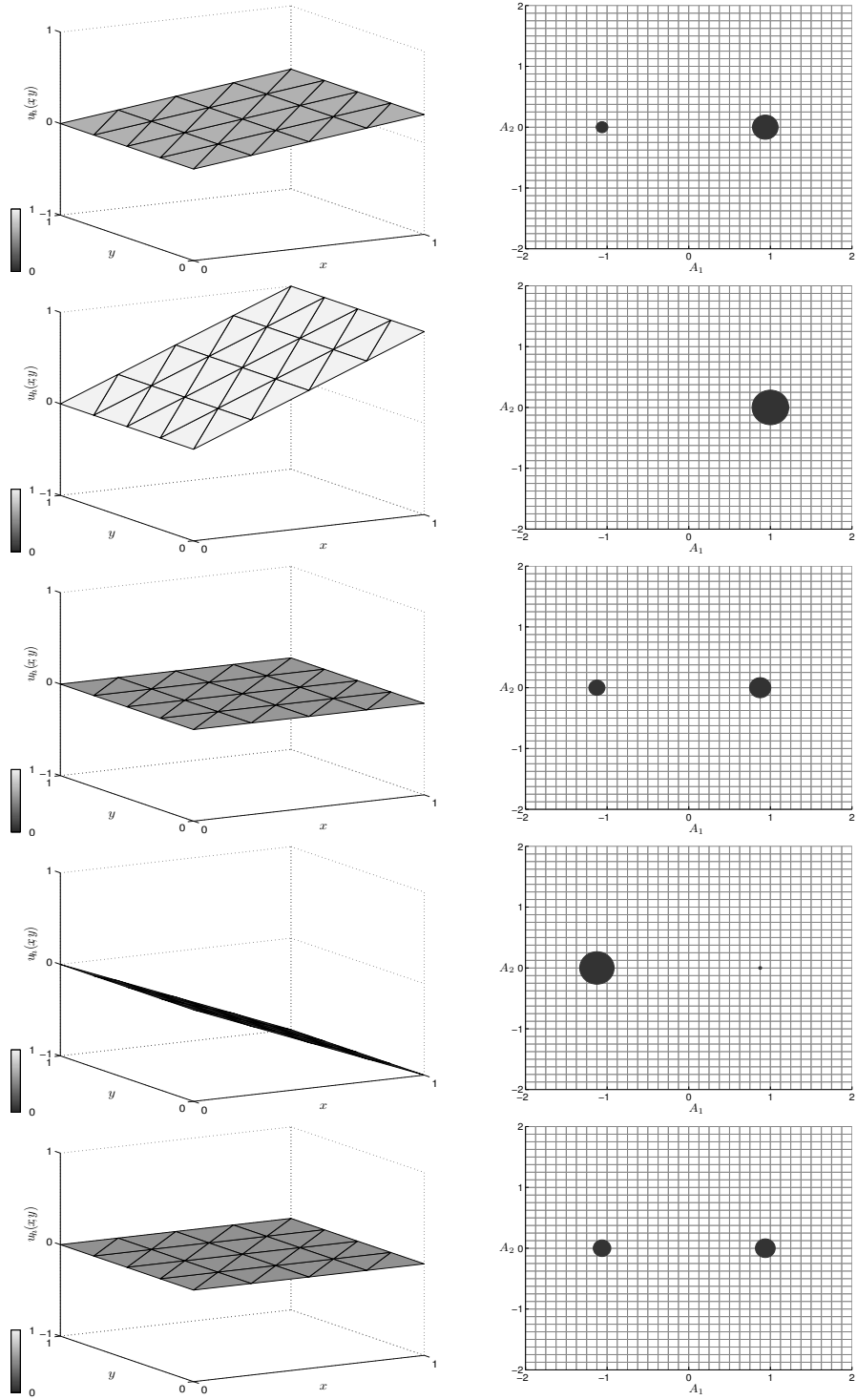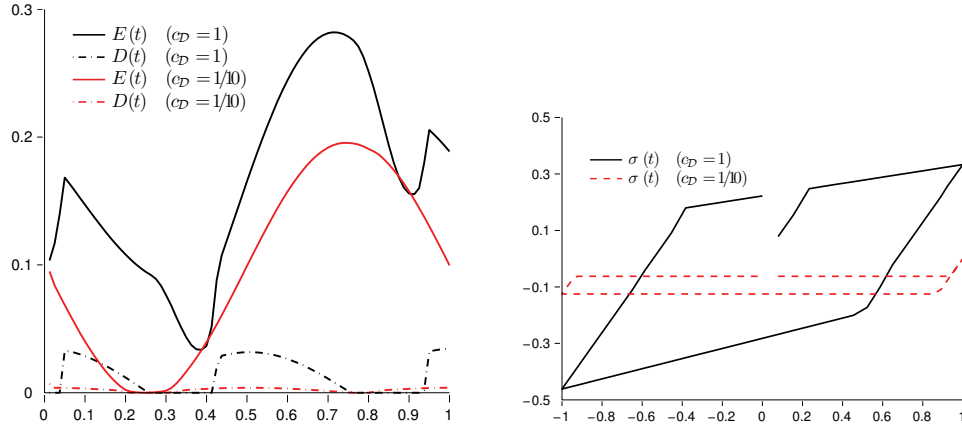
21

FIGURE 5. Scalar displacement $u_{j,h}$ (left) and discrete Young measure $\nu_{j,h}$ (right) for $j = 4, 20, 40, 60, 80$ in Example 4.1 with $c_{\mathcal{D}} = 1/10$. The displacement is coloured by the quantity λ_h and the sizes of the dots in the grid in the right plots are proportional to the volume fraction associated to a grid point. The grid indicates every second atom.

FIGURE 6. Total energy and dissipation as functions of $t \in [0,1]$ in Example 4.1 with $c_{\mathcal{D}} = 1$ and $c_{\mathcal{D}} = 1/10$ (left). Stress versus strain for $t \in [0,1]$ in Example 4.1 with $c_{\mathcal{D}} = 1$ and $c_{\mathcal{D}} = 1/10$ (right).
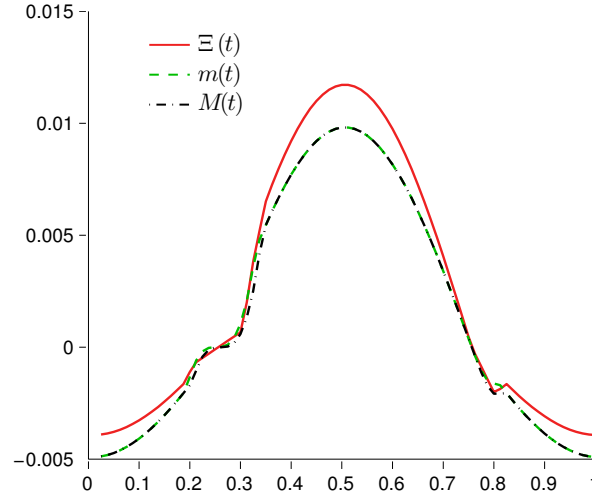

FIGURE 7. Experimental two-sided energy estimate in Example 4.1 for $c_{\mathcal{D}} = 1$.

For a triangulation of Ω consisting of 128 triangles, the set $\mathcal{A}_{d,r}$ defined through $d = 2^{-6}$ and $r = 3/2$, the time-step size $\tau = 1/20$, and the choice

$$c_{\mathcal{D}} = 1$$

Figure 9 shows snapshots of the evolution for $t = j/20$ with $j = 1, 5, 10, 20$.

Figure 8 displays the energy and the dissipation contribution, i.e., the quantities

$$E(t_j) = \sum_{T \in \mathcal{T}} |T| \sum_{A \in \mathcal{A}_{d,r}} \theta^j_{T,A} W(A) + D(t_j), \qquad D(t_j) = c_{\mathcal{D}} \sum_{T \in \mathcal{T}} |T| a_T(t_j)$$
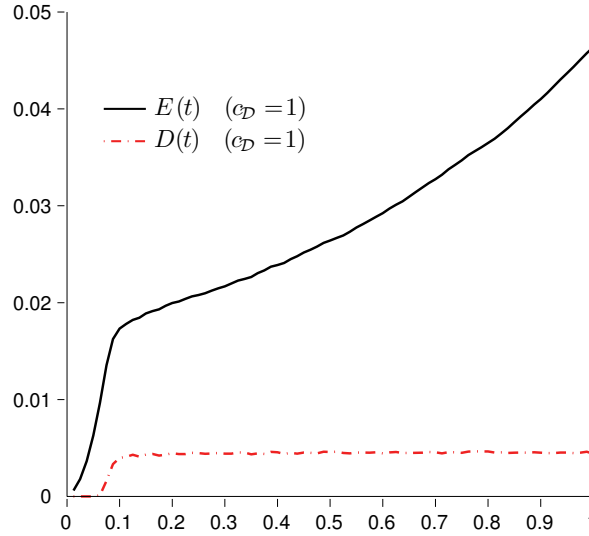
as functions of $t \in [0,1]$.

23

FIGURE 8. Total energy and dissipation as functions of $t \in [0, 1]$ in Example 4.3.

We found out that the proposed method works effectively. In fact, if we consider (ii) in Lemma 1.1 not only polyconvex functions but also for a finite number of quasiconvex ones, the related maximum principle provides an improved lower bound of the quasiconvex envelope. A further step might be to investigate wherther the polyconvex Young measure obtained by our algorithm is a laminate. These aspects are left for future research.

REFERENCES

[1] Arndt, M.: Upscaling from Atomistic Models to Higher Order Gradient Continuum Models for Crystalline Solids. PhD.Thesis, Inst. für Numer. Simulation, Universität Bonn, 2004.

[2] Aubin, J.-P., Ekeland, I.: *Applied Nonlinear Analysis.* New York, J. Wiley, 1984.

[3] Aubri, S., Fago, M., Ortiz, M.: A constrained sequential-lamination algorithm for the simulation of sub-grid microstructure in martensitic materials. *Comp. Meth. in Appl. Mech. Engr.* 192 (2003), 2823–2843.

[4] Ball, J.M.: Convexity conditions and existence theorems in nonlinear elasticity. *Arch. Rat. Mech. Anal.* **63** (1977), 337–403.

[5] Ball, J.M.: A version of the fundamental theorem for Young measures, In: *PDEs and Continuum Models of Phase Transition.* (M.Rascle, D.Serre, M.Slemrod, eds.) Lecture Notes in Physics 344, Springer, Berlin, (1989), pp. 207–215.

[6] Ball, J.M., James, R.D.: Fine phase mixtures as minimizers of energy. *Archive Rat. Mech. Anal.* **100** (1988), 13–52.

[7] Bartels, S.: Linear convergence in the approximation of rank-one convex envelopes. *M2AN, Math. Model. Numer. Anal.* **38** (2004), 811–820.
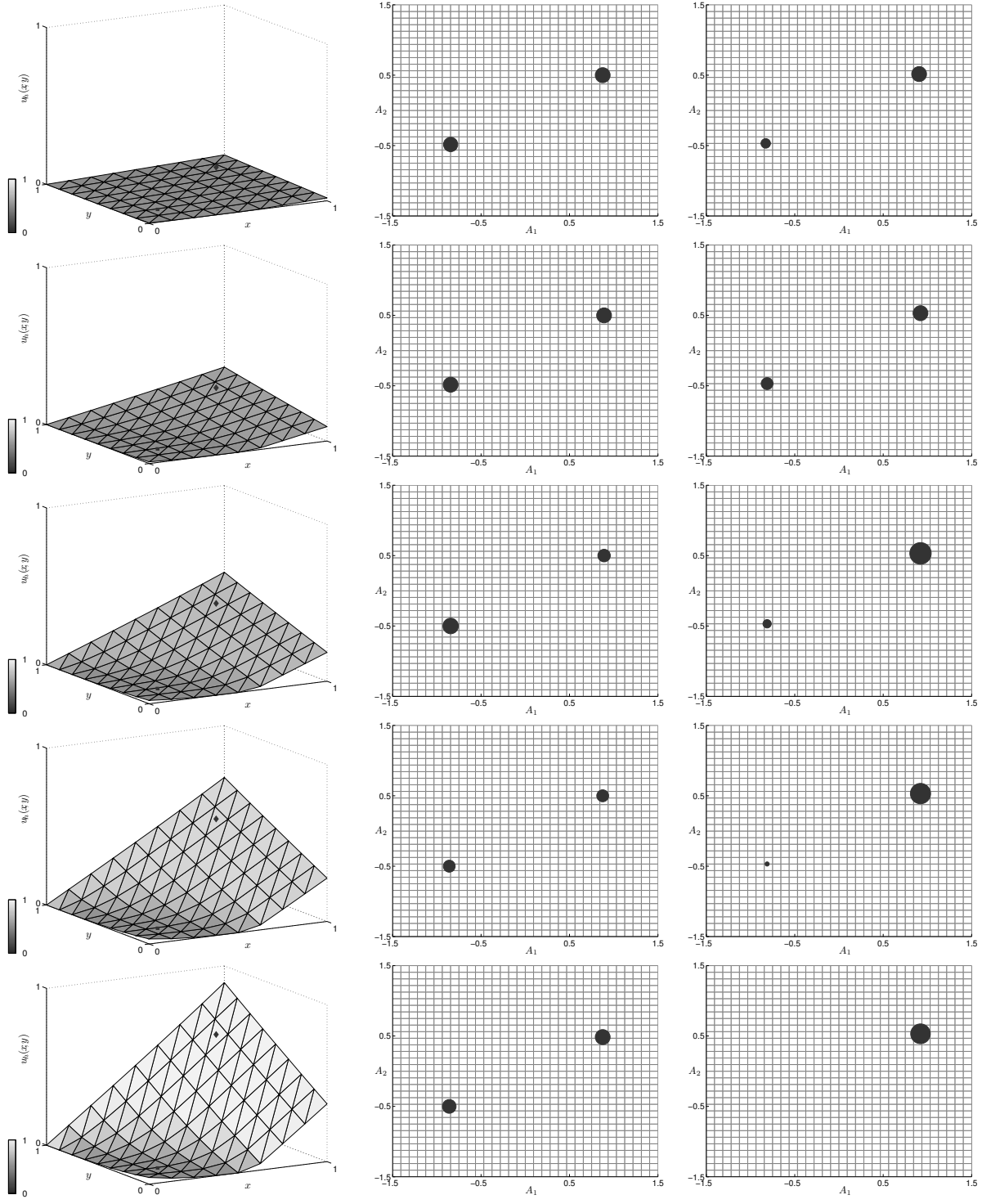
FIGURE 9. Scalar displacement $u_{j,h}$ (left) and discrete Young measure $\nu_{j,h}$ related to the elements indicated by the filled square (middle) and the filled diamond (right) for $j = 4, 20, 40, 60, 80$ in Example 4.3 with $c_\mathcal{D} = 1$. The displacement is coloured by the quantity σ_h; the sizes of the dots represent the volume fractions of every sixth atom.

25

[8] Bartels, S.: Reliable and efficient approximation of polyconvex envelopes. *SIAM J. Numer. Anal.* **43** (2005), 363–385.

[9] Carstensen, C., Roubíček, T.: Numerical approximation of Young measures in nonconvex variational problems, *Num. Math.* **84** (2000), 395–415.

[10] Dacorogna, B.: *Direct Methods in the Calculus of Variations*, Springer, Berlin, 1989.

[11] Dolzmann, G., Walkington, N.: Estimates for numerical approximations of rank one convex envelopes. *Numer. Math.* **85** (2000), 647–663.

[12] Ekeland, I., Temam, R.: *Convex Analysis and Variational Problems*, North-Holland, Amsterdam, 1976.

[13] Francfort, G., Mielke, A.: An existence result for a rate-independent material model in the case of nonconvex energies. *J. reine u. angew. Math.* **595** (2006), 55–91.

[14] Govindjee, S., Mielke, A., Hall, G.J., Miehe, C.: Application of notions of quasi-convexity to the modeling and simulation of martensitic and shape memory phase transformations. In: Proc. *5th World Congress on Computational Mechanics*, (H.A. Mang, F.G. Rammerstorfer, J. Eberhardsteiner, Eds), Vienna University of Technology, Austria, (2002)

[15] Hackl, K., Hoppe, U.: On the calculation of microstructure for inelastic materials using relaxed energies. In: IUTAM Symp. *Comput. Mech. of Solid Materials at Large Strains* (Ch.Miehe ed.), Kluwer, Dordrecht, 2003, pp.77–86

[16] Huo, Y., Müller, I.: Nonequilibrium thermodynamics of pseudoelasticity. *Continuum Mech. Thermodyn.* **5** (1993), 163–204.

[17] Kružík, M.: Maximum principle based algorithm for hysteresis in micromagnetics. *Adv. Math. Sci. Appl.* **13** (2003), 461485.

[18] Kružík, M., Mielke, A., and Roubíček, T.: Modelling of microstructure and its evolution in shape memory-alloy single-crystals, in particular in CuAlNi. *Meccanica* **40** (2005), 389–418.

[19] Kružík, M., Prohl, A., Young measure approximation in micromagnetics. *Num. Math.* **90** (2001), 291–307.

[20] Mielke, A., Roubíček, T.: Rate-independent model of inelastic behaviour of shape-memory alloys. *Multiscale Modeling Simul.* **1** (2003), 571-597.

[21] Mielke, A., Theil, F.: A mathematical model for rate-independent phase transformations with hysteresis. In: *Models of continuum mechanics in analysis and engineering.* (Eds.: H.-D.Alder, R.Balean, R.Farwig), Shaker Verlag, Aachen, 1999, pp.117-129.

[22] Mielke, A., Theil, F., Levitas, V.I.: A variational formulation of rate-independent phase transformations using an extremum principle. *Archive Rat. Mech. Anal.* **162** (2002), 137–177.

[23] Pedregal, P.: *Parametrized Measures and Variational Principles*, Birkhäuser, Basel, 1997.

[24] Roubíček, T.: Relaxation of vectorial variational problems. *Matematica Bohemica* **120** (1995), 411–430.

[25] Roubíček, T.: *Relaxation in Optimization Theory and Variational Calculus.* W. de Gruyter, Berlin, 1997.

[26] Roubíček, T.: Models of microstructure evolution in shape memory materials. In: NATO Workshop *Nonlinear Homogenization and its Appl. to Composites, Polycrystals and Smart Mater.* (Eds. P.Ponte Castaneda, J.J.Telega, B.Gambin), NATO Sci. Series **II/170**, Kluwer, Dordrecht, 2004, pp.269–304.

[27] Young, L.C.: Generalized curves and existence of an attained absolute minimum in the calculus of variations, *Comptes Rendus de la Société et des Lettres de Varsovie*, Classe III **30** (1937), 212–234.